DEUTSCHES ELEKTRONEN-SYNCHROTRON DESY

DESY 82-052
August 1982

MEASUREMENT OF R IN e^+e^- ANNIHILATION FOR $\sqrt{s}$ BETWEEN 7.4 AND 9.4 GeV

by

LENA Collaboration

NOTKESTRASSE 85 · 2 HAMBURG 52

To be sure that your preprints are promptly included in the HIGH ENERGY PHYSICS INDEX, send them to the following address (if possible by air mail) :

DESY
Bibliothek
Notkestrasse 85
2 Hamburg 52
Germany

DESY 82-052
August 1982

Measurement of R in e^+e^- Annihilation for $\sqrt{s}$ between 7.4 and 9.4 GeV.

LENA Collaboration

B. Niczyporuk, Z. Jakubowski, G. Nowak
Institute of Nuclear Physics, Cracow, Poland

G. Folger, B. Lurz, U. Volland, H. Wegener
Physikalisches Institut der Universität Erlangen-Nürnberg, Germany

J.K. Bienlein, R. Graumann, H.-J. Trost, M. Schmitz
Deutsches Elektronen-Synchrotron DESY, Hamburg, Germany

F.H. Heimlich, R. Nernst, A. Schwarz, U. Strohbusch, P. Zschorsch
I. Institut für Experimentalphysik der Universität Hamburg, Germany

K.W. Chen, A.C. König, D.J. Schotanus
University of Nijmegen and NIKHEF-Nijmegen, The Netherlands[1]

M. Coles, A. Engler, R.W. Kraemer, D. Marlow, F. Messing, C. Rippich, S. Youssef
Department of Physics, Carnegie-Mellon University, Pittsburgh, USA[2]

A. Fridman
DPhPE, Centre d'Etudes Nucléaires de Saclay, Gif sur Yvette, France

G. Alexander, A. Av-Shalom, G. Bella, J. Grunhaus
Department of Physics and Astronomy, Tel-Aviv University, Israel[3]

M. Scheer
Physikalisches Institut der Universität Würzburg, Germany

---

1 partially supported by FOM-ZWO
2 partially supported by the US Department of Energy
3 partially supported by the Israeli Academy of Sciences and Humanities - Basic Research Foundation

Abstract

The ratio $R = \sigma(e^+e^- \to \text{hadrons})/\sigma(e^+e^- \to \mu^+\mu^-)$ was measured with the LENA detector at DORIS in a scan between 7.40 and 7.48 GeV and between 8.67 and 9.43 GeV center of mass energies. Corrected for QED radiative effects, R is found to be constant with an average value of $R=3.37\pm0.06_{stat.}\pm0.23_{syst.}$ No narrow resonances with $\Gamma_{ee}\cdot(\Gamma_{had}/\Gamma_{tot})\geq 0.30$ keV (95% C.L.) and no steps have been observed. Based on this value of R, revised values for $\Upsilon(1S)$ resonance parameters are presented.

1. Introduction

In this paper we present results of a measurement of the total hadronic cross section $\sigma(e^+e^-\rightarrow\text{hadrons})$ in the energy region below the Υ resonances using the LENA detector at the e^+e^- storage ring DORIS. Data were taken in fine energy steps between center of mass energies of 7.40 and 7.48 GeV and between 8.67 and 9.43 GeV. Data taking took place between July and October 1980 and an integrated luminosity of 1141 nb^{-1} has been collected.

The ratio R is defined as $\sigma(e^+e^-\rightarrow\text{hadrons})/\sigma(e^+e^-\rightarrow\mu^+\mu^-)$ where both cross sections are lowest order in QED and the hadronic cross section does not include any contribution from τ-pair decays. In the quark model the process $e^+e^-\rightarrow$hadrons proceeds via an intermediate quark pair which subsequently fragments into hadrons. R is a measure of the sum of the squares of the quark charges. With the emergence of QCD as a viable theory of the strong interactions, deviations from the simple quark model picture were expected. Expressions for first and second order QCD corrections to R have been derived [1]. It has been argued that a measurement of R in an energy range well above the charm resonances and below the bottom resonances would form the best quantitative test of QCD [2,3]. This is based on the expectation that in this energy region QCD corrections are small enough to be treated perturbatively and still large enough to be measurable.

Until recently no single experiment measured R in fine steps spanning the energy range between the charm and the bottom resonances. On the low energy side measurements of R have been performed by the SLAC-LBL collaboration with the Mark I detector at SPEAR [4] and on the high energy side by the PLUTO [5] and D-HH-HD-M [6] groups at DORIS. The SLAC-LBL (Mark I) results, which showed an R value increasing with energy, seemed hard to reconcile with QCD predictions [2]. This has given rise to speculations about additional thresholds or "new physics" phenomena appearing in this energy range. All this made it very interesting to cover the region mentioned above with a single experiment. If no new phenomena or resonances are encountered one has a good QCD test since the absence of resonances greatly simplifies the QCD as well as the QED analysis of the results.

In this experiment 95 data points were taken in a fine energy scan between 7.40 and 7.48 GeV and between 8.67 and 9.43 GeV center of mass energies. The step size for the energy scan was chosen equal to the DORIS machine resolution (proportional to E^2) resulting in E_{CM} steps ranging from 6 MeV at 7.4 GeV to 10 MeV at 9.4 GeV. Since the experiment was intended to be sensitive to resonances with an electronic width as small as one third that of the $\Upsilon(1S)$ resonance, we aimed at about 50 hadronic events per energy

point. Due to beam-time limitations this number was halved for the second part of the experiment.

The outline of this paper is as follows. In section 2 we describe our apparatus and trigger conditions. In section 3 we outline the experimental determination of R. Sections 4 and 5 deal with hadronic events, in sections 6 and 7 we discuss large angle Bhabha events and luminosity. In section 8 we deal with τ-pair and $\gamma\gamma$ subtraction. Section 9 is reserved for summary and conclusions.

2. Apparatus

Figure 1 shows the non-magnetic LENA detector used at DORIS [7]. Starting at the interaction point a particle first traverses a 0.06 radiation length aluminum beam pipe followed by three double layers of cylindrical drift chambers. Each double drift chamber has 128 anode wires to measure the azimuthal coordinates and 80 cathode strips to measure the polar angle coordinates of a charged track. The correlation between cathode and anode signals is accomplished by comparing the drift times on the anode wires with the times of the induced signals on the cathode strips. External to the first and third drift chambers are 32 element trigger scintillation hodoscopes. Between the second and third drift chamber there is a one radiation length thick (as viewed from the interaction region) lead sheet consisting of two partial cylinders which together cover 75% of the full azimuthal angle. The inner detector consisting of the drift chambers and hodoscope assembly has a solid angle coverage of 86% of 4π sr.

Surrounding the inner detector is the energy detector which has 178 blocks of sodium iodide (NaI) or lead glass. The NaI blocks are situated behind the gaps in the lead converter. They consist, in part, of a 1.8 radiation length thick segmented active converter which converts gamma rays with high efficiency and energy resolution. Planar drift chambers and plastic scintillation counters (converter hodoscopes) are used for measuring the conversion point and triggering on photons. Beyond the active converter are NaI blocks followed by lead glass blocks. The sidewalls have a total thickness of 16.2 radiation lengths at normal incidence. The lead glass arrays above and below the inner detector are 12.7 radiation lengths thick at normal incidence, and the irregularly shaped blocks between the side wall and the top and bottom assemblies are between 6 and 10 radiation lengths thick depending on the azimuthal angle of incidence. The NaI and lead glass blocks give energy information for approximately 80% of 4π sr. Surrounding the energy detector are time of flight counters and muon range counters consisting of steel absorber followed by drift chambers and time of flight counters.

The charged particle angular resolution in the drift chambers was determined by using cosmic ray muons. The r.m.s. resolution in the azimuthal angle φ is 15 mrad and in the polar angle ϑ the r.m.s. resolution is $\delta(\cot\vartheta)=0.07$. The lead glass and NaI blocks are used to determine the energies of the electrons and photons. The energy detector was calibrated by minimizing the width of the energy distribution of large angle Bhabha events. The energy resolution of the detector was then determined from two photon final state events to be $\sigma_E/E = 6\%$ for 4.7 GeV photons in the thick regions of the detector. A block to block comparison was made from the energies deposited per track length by cosmic particles.

The detector was triggered by a multiple coincidence between elements of the two hodoscope layers of the inner detector at the same azimuthal angle plus a requirement on the amount of energy deposited. Each coincidence within the inner detector defined a track. Different amounts of energy were required in the energy detector, depending on the multiplicity of tracks within the inner detector. If three or more tracks were found, the energy deposition required for a trigger was roughly 250 MeV. If one or two tracks were found, the energies needed were 800 MeV or 300 MeV respectively. If no tracks were observed in the inner detector, we required a signal in at least one of the outer hodoscopes or converter hodoscopes plus at least 1 GeV of energy deposited. The trigger efficiency was determined to be greater than 99.9%. A special μ-pair trigger was also available. We made use of a PDP 9 on-line computer to reject events which did not contain radial drift chamber tracks corresponding to hodoscope tracks. In this way we immediately discarded many cosmic, beam gas and beam wall events.

The luminosity was measured in two independent ways. A luminosity monitor measured small angle Bhabha events which had a central scattering angle of 130 mrad. Large angle Bhabha events (defined by $|\cos\vartheta|<0.8$) were identified in the drift chambers and energy detector.

3. Procedure.

Normalizing the hadronic events to large angle Bhabha scattering, we obtain the visible hadronic cross section:

$$\sigma_H^{vis} = \sigma_B^{vis} \frac{N_H\ (1-\Delta_H)}{N_B\ (1-\Delta_B)} .$$

N_H and N_B are the numbers of observed hadronic and large angle Bhabha events, respectively. Δ_H corrects for the cosmic, single beam and Bhabha background in the hadronic sample. Δ_B accounts for cosmic and single beam background in the large angle Bhabha sample. σ_B^{vis} is a Monte Carlo calculation of the visible large angle Bhabha cross section and includes radiative corrections calculated using the method of Berends and Kleiss [8].

As we are interested in hadron production via one-photon exchange giving a quark pair, we have to subtract the contributions due to τ-pairs and due to $\gamma\gamma$ (two-photon) reactions from the visible hadronic cross section:

$$\sigma_{H,1\gamma}^{vis} = \sigma_H^{vis} - \sigma_\tau^{vis} - \sigma_{\gamma\gamma}^{vis} .$$

Radiative corrections to the one-photon exchange hadronic cross section have been applied using the method of Berends and Kleiss [8]:

$$\sigma_{H,1\gamma}^{vis} = \sigma_H^0 \int_0^{k_{max}} dG/dk \cdot \varepsilon(k) \cdot dk$$

$$\equiv \sigma_H^0 \cdot Q$$

where

σ_H^0 is the lowest order QED hadronic cross section which we want to determine,

$k = E_{\text{initial state photon}}/E_{\text{beam}}$,

$k_{max} = 1 - (m_\pi/E_{beam})^2$,

$\varepsilon(k)$ is the detection efficiency for hadronic events.

The function G(k) is explicitly derived in [8] and includes the vertex correction and initial state radiation as well as e, μ, τ and hadronic vacuum polarization.

We define the integral Q as the acceptance of the experiment. It comprises the geometrical, trigger and event selection efficiencies ($\varepsilon(k)$) as well as the radiative corrections (dG/dk).

Since $R \equiv \sigma_H^0/\sigma_\mu^0$, we have

$$R = (\sigma_H^{vis} - \sigma_\tau^{vis} - \sigma_{\gamma\gamma}^{vis}) / (\sigma_\mu^0 \cdot Q) .$$

σ_μ^0 is calculated in QED, σ_τ^{vis} and $\sigma_{\gamma\gamma}^{vis}$ are determined by Monte Carlo calculations based on what is known about τ decays and $\gamma\gamma$ collisions. Q is calculated by a Monte Carlo integration using a jet model of quark fragmentation [9].

4. Hadronic Event Selection

A central problem of the R measurement was the selection of the hadronic events. This was difficult because there were about 1000 background events for every hadronic event written to tape. In order to have a small background, the event selection procedure should accept less than approximately one background event out of 100,000. In this section, we describe the gross features of the background, the method of event selection, and our estimate of the background in the hadronic sample.

Most of the background events were caused by interactions of electrons or positrons with the beam pipe or with residual gas molecules (collectively called single beam events). A smaller part of the background was events caused by cosmic ray particles. Both backgrounds were characterized by non-radial tracks, low energy tracks which may stop in the inner detector, tracks which deposit small energies in the energy detector, and events which were very asymmetric. These characteristics of the background events were used to distinguish them from true hadronic events.

Hadronic events were selected by a computer program which imitated the reasoning previously used in our visual scans for hadronic events [10]. Events were seldom accepted or rejected for a single reason. The framework for making the selection was that seventeen quantities called "indicators" were calculated for each event. Each indicator was a measure of the goodness of an event and also corresponded to a visual scan criterion. Events were accepted or rejected depending on the value of the sum of the indicators. Minimal requirements for an event to be accepted included requiring at least three charged tracks in the inner detector and requiring at least 1100 MeV visible energy (600 MeV for the center of mass energy region 7.4 to 7.5 GeV).

Details of the event selection can be found in [11]. Here we briefly describe two of the seventeen indicators. One indicator was made from the fraction of visible energy in the active converter. If this fraction was large, it indicated many stopping particles or particles travelling nearly parallel to the beam axis. This variable indeed gave useful discrimination against single beam events. A more complicated indicator was calculated from the number of drift chamber hits assigned to tracks compared with the number left unassigned. Only radial drift chamber hits were assigned to tracks and so this indicator discriminated against events which had tracks originating far from the axis of the detector.

The background in the hadronic sample was estimated by allowing the program to select events from single beam runs and cosmic (no beam) runs. Results were checked by a visual scan of the selected events. The

resulting backgrounds were (1.5±0.5)% for a visible energy cut of 1100 MeV in the 8.6 to 9.4 GeV data and (4.0±1.0)% for a cut of 600 MeV in the 7.4 to 7.5 GeV data.

Requiring radial tracks implied that the interaction vertex was within 40 mm radius of the detector axis. Upon reconstruction, we found that all the selected hadronic events had vertices within a cylinder of radius 5 mm. We also checked that the distribution of event vertices along the beam axis was smooth and symmetric and did not have long tails indicative of background.

During the analysis of the primary data we found an error in the on-line data acquisition program which caused events with tracks passing through certain cathode strips at one end of the detector to be rejected. A correction factor was derived using the cathode strips at the opposite end of the detector. For hadronic events this correction factor is +(5.3±0.6)%.

The method of event selection described here was a major improvement over earlier methods. Because of the efficient elimination of background events, we were able to decrease the visible energy requirement from 1800 MeV to 1100 MeV (or to 600 MeV for 7.4 to 7.5 GeV). Because the energy cut has been decreased, the efficiency for hadronic events increased from 65% to 85% (at 9 GeV with no radiative corrections). Since the event selection procedure involves no human intervention, reliable efficiencies and backgrounds can be calculated.

5. Monte Carlo Simulation of Hadronic Events

The acceptance, Q, was calculated by Monte Carlo integration. Recall that

$$Q \equiv \int dG/dk \cdot \varepsilon(k) \cdot dk$$

where all quantities have previously been defined (section 3). The acceptance depends on the maximum photon energy generated. Since an initial state radiation produces hadronic events at lower center of mass energies, the acceptance depends also on R(s). To obtain Q we first generated an initial state photon according to the functions given by Berends and Kleiss [8]. Then hadrons were generated according to the LUND 1980 version of the extended Field-Feynman quark-antiquark fragmentation scheme [9]. We used the default LUND parameters with two exceptions: we set the ratio of primary vector mesons to all primary mesons equal to 0.4 and we used a charm fragmentation function proportional to z.

Given a set of four-vectors, these Monte Carlo events were then subjected to detector simulation. Some gross features of this Monte Carlo are:

- Simulation of the response of the drift chambers to charged particles including multiple scattering. The cathode strips of the inner detector were somewhat noisy and special effort went into this part of the algorithm.
- Minimum ionizing particles deposit energy according to their track length. Stopping charged hadrons and charge exchange reactions are simulated.
- Electrons and photons deposit energy according to an approximate empirical formula [12]. Photon conversion is simulated in the beam pipe and all parts of the detector.

The acceptance Q as a function of E_{CM} is shown in Figure 2. The acceptance increases smoothly from 0.82 to 0.90 between 7.4 and 9.4 GeV.

To estimate the systematic uncertainty in Q we first established that the Monte Carlo simulation well represents the relevant aspects of the data. Then we varied the Monte Carlo parameters to establish the systematic uncertainty associated with each parameter. The amount that each parameter was varied was guided either by information from our own experiment or from other measurements [13].

In Figure 3 we compare the distributions of the visible energy and the charged multiplicity of the data with the Monte Carlo results. Agreement between data and simulation is good. We also checked the distribution in $\Delta\varphi$, the difference between azimuthal angles of neighboring tracks in the

hadronic sample. Again Monte Carlo events gave an adequate representation of the data.

The parameters of the jet generation program are especially important. For all but the charm fragmentation function and the fraction of vector mesons produced, we have varied these parameters according to the uncertainties in [13]. The change in Q is negligible. There is some indication that the charm fragmentation function rises with z. The variation of Q as the charm fragmentation function is changed from constant to a form proportional to z^2 is 1.0%. This we take as a contribution to the systematic error. By requiring that the Monte Carlo multiplicity distributions give an adequate fit to the data, we were able to restrict the range of the vector meson parameter to between 0.35 and 0.40. The corresponding variation in Q is 1.3%.

We also calculated the acceptance, Q, using the LUND 1981 (version 4.1) hadronic event generator [9] which includes baryon production. Using the default parameter values, the same acceptance as a function of energy was found.

Q depends on the shape of R(s) at all energies below the center of mass energy. We found, however, there is only a 0.1% difference in Q between a constant R(s) and a step function where R(s) is taken zero below charm threshold. We also found that Q is independent of low energy resonances like the J/Ψ. We conclude that any dependence of Q on R(s) is negligible.

Although the initial state radiation calculations of Berends and Kleiss describe the μ-pair data very well [14], we attribute a 1% systematic error to the acceptance due to higher order radiative corrections and uncertainty in the hadronic vacuum polarization [15]. Calculations have shown the effect of final state radiation to be of the order of 0.02% [16].

The energy calibration (see section 2) has shown a 5% overall and a 8% block to block uncertainty in the energy. The corresponding variations in Q are 2.2% and 2.7%, respectively, giving a 5% systematic uncertainty coming from energy calibration. To account for the effects of noise in the detector which we were not able to simulate in the Monte Carlo program, we assign a 1.3% systematic error to Q based crudely on the number of events which are close to failing (but do not fail) the event selection program.

We have varied along the beam direction the peak of the vertex distribution by an amount equal to twice its observed width and find the acceptance varies by 1%.

It is important to point out that the hadronic event selection program is quite insensitive to the fine details of the Monte Carlo simulation of an event in the detector. For example, the information we use from the energy detector is the total visible energy, the fraction of energy deposited in the active converter and whether a charged track has any energy associated with it. Moreover, the inclusion of charge exchange reactions in the simulation of the energy deposition has a negligible effect on the acceptance.

In Table 1 we summarize the contributions to the systematic uncertainty in the acceptance Q. We have added these errors in quadrature and the result is 5.6%.

6. Large Angle Bhabha Event Selection

In contrast to the hadronic event selection, the large angle Bhabha event selection can be motivated by a few simple considerations. When an electron which had nearly the full beam energy entered our energy detector, it showered and deposited a large fraction of it's total energy (typically 2000 to 4000 MeV). A charged hadron deposited only about 200 MeV in the energy detector. As a result, large angle Bhabhas were easily distinguished from hadronic events. Because of their high energy concentrated in two tracks, there was virtually no background expected from cosmic or single beam events. Another feature of the large angle Bhabha events was that the cross section rises rapidly as the polar angle decreases. This meant that there were edge effects and so the polar angle cut had to be done with care.

The large angle Bhabha event selection program was fairly conventional (i.e., cuts instead of indicators as in the hadronic selection) except that all the tracking variables and energy clustering were optimized for this channel. The accepted large angle Bhabha events satisfied the following requirements. Each event had exactly two tracks in the φ dimension of the drift chambers and one, two, or three tracks in the cathode strips. The tracking in the φ dimension was such that only one track was counted even if the particle showered in the beam pipe. The tracks satisfied $|\cos\vartheta|<0.7$ (where ϑ is the polar angle). The φ acollinearity between the two tracks was less than 14 degrees. The energy associated with each of the tracks was between 600 MeV and 7 GeV and the total visible energy was between 2 and 12 GeV. Figure 4 shows distributions of the energies of the large angle Bhabha tracks. The substantial widths and the shifts in the peaks of these distributions were due to the different thicknesses of various parts of the energy detector. Figure 5 shows the polar angle distribution of the large angle Bhabha tracks with an angle cut of $|\cos\vartheta|<0.8$. The $|\cos\vartheta|<0.8$ cut was used to check our sensitivity to the obvious edge effect shown in Figure 5 (tracks with $|\cos\vartheta|>0.8$ result from the averaging procedure required because of the finite widths of the cathode strips). Luminosities calculated with either angle cut are consistent. For the final results, we used the $|\cos\vartheta|<0.7$ cut because fewer events are near the edge of the distribution. For both the $|\cos\vartheta|<0.7$ and 0.8 cuts, the φ distributions were found to be flat.

To determine the background in the large angle Bhabha sample, the selection program was run on single beam and cosmic data. After normalization, the background was found to be 0.1%. To check this result, an unbiased sample of 190,000 colliding beam triggers was passed through our event selection program. 539 events were accepted and these were visually searched for possible background. No background event was found which

gives a 90% C.L. of 0.4% for the size of the background. This upper limit is consistent with the previous estimate.

The loss of events due to the error in the on-line data acquisition program was corrected for in the same manner as in the hadronic event sample. This correction to N_B is +(0.36±0.07)%.

7. Large Angle Bhabha Visible Cross Section

At a particular center of mass energy, the luminosity $\mathcal{L}$ is given by

$$\mathcal{L} = N_B / \sigma_B^{vis}$$

where N_B is the number of accepted Bhabha events and σ_B^{vis} is the corresponding cross section. We calculated this cross section by Monte Carlo integration. Bhabha final states were generated by a Monte Carlo program which included radiative corrections up to order α^3. The final state was then simulated in the detector as described in section 4. The visible cross section was calculated using

$$\sigma_B^{vis} = \sigma_B^{generated} \cdot \varepsilon_B$$

where $\sigma_B^{generated}$ is calculated from QED [8], and ε_B is the detection and selection efficiency. The result is:

$$\sigma_B^{vis} = 11.64\ \sigma_\mu^0 \ .$$

With a method similar to that used for the hadronic acceptance Q, the systematic uncertainty in the visible Bhabha cross section was calculated by varying parameters in the Monte Carlo simulation. Table 2 summarizes these contributions. Simulation of the observed Bhabha total energy distribution gave a 1.5% systematic uncertainty. The entry "Shower Shapes" refers to the uncertainty we associated with our method of shower simulation. We have added the systematic errors for "Detector Noise", "Shower Shapes", "Vertex Position" and "Cathode Strip Simulation" linearly because of the uncertainties in the estimates of those errors. Then the errors were taken in quadrature and the resulting uncertainty is 3.4%.

An analysis of the Bhabha events in our small angle luminosity monitors showed agreement with the large angle Bhabha results to within 4% but with a 10% systematic error. For the final results, we used the large angle Bhabha luminosities.

We collected a total integrated luminosity of 1141 nb^{-1}.

8. τ-Pair and Two-Photon Subtractions

Both the visible τ-pair and the visible $\gamma\gamma$ cross sections must be subtracted from the visible hadronic cross section. Monte Carlo estimates were made for both of these processes.

We generated τ-pair events using the standard V-A matrix element with hadronic branching fractions calculated by Kawamoto and Sanda [17] which are consistent with results thus far measured. Initial state radiation was handled in the same way as for the hadronic events (see section 3). The systematic error in the τ-pair subtraction was dominated by uncertainty in high multiplicity decay modes (9%) and in the energy calibration (3.5%). Adding these in quadrature, the total systematic error is 10% and we find

$$\sigma_\tau^{vis}/\sigma_\mu^0 = 0.260\pm0.026 \ , \ (E_{vis}>1100 \text{ MeV})$$

$$= 0.325\pm0.032 \ , \ (E_{vis}> 600 \text{ MeV}) \ .$$

These results do not significantly depend on the center of mass energy.

To estimate the visible hadronic cross section from the $\gamma\gamma$ collision process, we used the QED calculations of Bonneau, Gourdin and Martin [18] as described in the work of Field [19]. For the hadronic cross sections we used the results of the TASSO group [20]. Integration over the product of the QED luminosity function, hadronic cross section, and detector efficiency gives

$$\sigma_{\gamma\gamma}^{vis} = (0.026\pm0.007) \text{ nb}$$

where the 25% systematic error reflects the uncertainty reported for the TASSO results. The beam energy dependence of the luminosity function is $\log^2(2\cdot E_{beam}/m_{electron})$ and this factor changes by a negligible amount over our energy range. $\sigma_{\gamma\gamma}^{vis}$ is less than 1% of the visible hadronic cross section; the uncertainty contributes a systematic error of only 0.2% to R.

9. Summary and Conclusions

We now have all the information needed to calculate R,

$$R = (\sigma_H^{vis} - \sigma_\tau^{vis} - \sigma_{\gamma\gamma}^{vis}) \ / \ (\sigma_\mu^0 \cdot Q) \ .$$

The systematic errors are collected in Table 3. The total systematic error is 6.7%. Figure 6 shows R as a function of E_{CM}. The details are tabulated in the Appendix.

As seen from Figure 6 no obvious resonances or steps are present. To search for narrow resonances we fitted a radiatively corrected Breit-Wigner for an hypothetical resonance to the measured cross sections. Each point in turn was taken to be the center of a resonance. We determined the upper limit for $\Gamma_{ee}\cdot(\Gamma_{had}/\Gamma_{tot})$ of a possible resonance to be 0.30 keV (95% C.L.).

In the absence of significant resonances we fitted a constant to the R values. We find R = 3.37±0.06. Allowing a linear energy dependence in the fit gave no improvement of χ^2. In particular there is no step in R between the 7.5 GeV region and the 8.7 to 9.4 GeV range. Table 4 presents R in four energy regions. Since there is no step between any of these regions we combine our results into a single R value between 7.4 and 9.4 GeV center of mass energy:

$$R = 3.37\pm0.06_{stat.}\pm0.23_{syst.} \ .$$

Our result on R is in agreement with QCD assuming four quark flavors and three quark colors in our energy region. From the theoretical first order formula,

$$R = 10/3 \cdot (1+\alpha_s/\pi),$$

we get the limit:

$$\alpha_s \leq 0.31 \text{ (68\% C.L.)}$$

This is not changed by using second order QCD formulas. The limit is consistent with our previously reported value $\alpha_s = 0.16^{+0.04}_{-0.02}\pm0.01$ [10] deduced from the $\Upsilon(1S)$ decay width.

The absence of any steps in the energy region covered excludes the threshold for production of a $\frac{2}{3}$ charged quark since this would give a step of $\Delta R = \frac{4}{3}$ (see Table 4). In a similar way we exclude a singly charged heavy lepton which decays mainly hadronically. The consistency of our data with

QCD also excludes the production of such particles below the energy range covered.

In Figure 7 we show a compilation of other R measurements made near our center of mass energy range.

Previously we have reported [10] measurements of $\Upsilon(1S)$ resonance parameters wherein we made use of the R value as determined by the PLUTO collaboration [5]. Based on the value of R presented here, we find $B_{\mu\mu} = (3.8\pm1.5\pm0.2)\%$, $\Gamma_{ee} = (1.13\pm0.09\pm0.08)$ keV and $\Gamma_{tot} = (30^{+20+3}_{-10-4})$ keV.

Acknowledgements

We acknowledge the efforts of the DORIS machine group, in particular Dr. K. Wille, and services rendered by the DESY staff. Our thanks are also due to the DESY-Heidelberg group which built the detector. We thank F.A. Berends and R. Kleiss for helpful discussions concerning the QED radiative corrections. The non-DESY members of the collaboration thank the DESY directorate for its hospitality. A.A., B.N. and Z.J. would like to thank the DESY directorate for financial support.

References

1. M. Dine and J. Sapirstein, Phys. Rev. Lett. 43, 668 (1979),
   K.G. Chetyrkin, A.L. Kataev and F.V. Tkachov, Phys. Lett. 85B, 277 (1979),
   W. Celmaster and R.J. Gonsalves, Phys. Rev. Lett. 44, 560 (1980).

2. R.M. Barnett, M. Dine and L.McLerran, Phys. Rev. D 22, 594 (1980).

3. J.D. Bjorken, Proceedings of the International Conference on High-Energy Physics, Geneva, pp. 245; ed. A. Zichichi (CERN, Geneva, 1979),
   H. Harari, Proceedings of the 1979 International Symposium on Lepton and Photon Interactions, Batavia, pp. 198; ed. T.B.W. Kirk and H.D.I. Abarbanel (Fermilab, Batavia, 1979),
   S.D. Drell, Proceedings of the 1981 International Symposium on Lepton and Photon Interactions at High Energies, Bonn, pp. 1003; ed. W. Pfeil Physikalisches Institut, University of Bonn, 1981).

4. J.L. Siegrist, Ph. D. Thesis, SLAC report SLAC-225 (1979),
   J.L. Siegrist et al., SLAC preprint SLAC-PUB-2831 (1981).

5. PLUTO Collab.,C. Berger et al., Phys. Lett. 81B, 410 (1979),
   Ch. Gerke, Dissertation, University of Hamburg (1979), report DESY PLUTO-80/03 (1980), unpublished.

6. DESY-Hamburg-Heidelberg-MPI München Collab., P. Bock et al., Z. Physik C 6, 125 (1980).

7. W. Bartel et al., Phys. Lett. 66B, 489 (1977),
   W. Bartel et al., Phys. Lett. 77B, 331 (1978).

8. We thank F.A. Berends and R. Kleiss for use of their Bhabha program,
   F.A. Berends and R. Kleiss, Nucl. Phys. B178, 141 (1981),
   F.A. Berends and R. Kleiss, Nucl. Phys. B177, 237 (1981),

9. R.D. Field and R.P. Feynman, Nucl. Phys. B136, 1 (1978),
   T. Sjöstrand, Lund report LU TP 80-3 (1980),
   T. Sjöstrand, Lund report LU TP 82-3 (1982).

10. LENA Collab., B. Niczyporuk et al., Phys. Rev. Lett. 46, 92 (1981).

11. S. Youssef, Ph. D. Thesis, Carnegie-Mellon University (1982), unpublished,
    S. Youssef et al., to be published.

12. G. Abshire et al., Nucl. Instr. and Meth. 164, 67 (1979).

13. TASSO Collab., R. Brandelik et al., Phys. Lett. 94B, 437 (1980).

14. For a review see A. Böhm, Physikalisches Institut der RWTA Aachen, report PITHA 81/30 (1981).

15. R. Kleiss, private communication.

16. F.J. Ynduráin, Nucl. Phys. B136, 533 (1978).

17. N. Kawamoto and A.I. Sanda, Phys. Lett. 76B, 446 (1978).

18. G. Bonneau, M. Gourdin and F. Martin, Nucl. Phys. B54, 573 (1973).

19. J.H. Field, Nucl. Phys. B168, 477 (1980); erratum, Nucl. Phys. B176, 545 (1980).

20. TASSO Collab., E. Hilger, DESY report 80/75 (1980).

21. S. Weseler (DASP II), Diplomarbeit, University of Heidelberg, report IHEP-HD/ARGUS/81-3 (1981),
    DASP II Collab., H Albrecht et al., report DESY 82/037 (1982).

22. CUSB Collab., E. Rice et al., Phys. Rev. Lett. 48, 906 (1982).

Table Captions

1. Systematic error in the acceptance Q (only significant sources are listed).

2. Systematic error in the luminosity.

3. Contributions to the systematic uncertainty in R.

4. R values in four energy regions and the combined result.

Table 1. Systematic Error in the Acceptance Q

Source of Uncertainty	Variation in Q (%)
Energy Calibration	5.0
Charm Fragmentation Function	1.0
Fraction of Primary Vector Mesons	1.3
Higher order Radiative Corrections and Hadronic Vacuum Polarization	1.0
Detector Noise Not Simulated in the Monte Carlo	1.3
Vertex Distribution	1.0
Sum in quadrature	5.6 %

Table 2. Systematic Error in the Luminosity

Source of Uncertainty	Variation in the Luminosity (%)
Energy Calibration	1.5
Shower Shapes	1.0
Higher Order Radiative Corrections	1.0
Vertex Position	0.6
Detector Noise not Simulated in the Monte Carlo	0.7
Cathode Strip Simulation	0.6
Monte Carlo Statistics	0.3
Center of Mass Energy Dependence	0.2
Background Subtraction	0.1
Result (see text)	3.4 %

Table 3. Summary of the Systematic Uncertainties in R

Source of Uncertainty	Variation in R (%)
Acceptance (Q)	5.6
Luminosity	3.4
τ Subtraction	0.9
On-line Data Acquisition	0.7
Background in the Hadronic Sample	0.5
Two Photon Subtraction	0.2
Sum in Quadrature	6.7 %

Table 4. R values in four energy regions and the combined result.

E_{CM} (GeV)	N_H	Lum. (nb^{-1})	$R \pm \Delta R_{stat.}$
7.40-7.48	830	172	3.37±0.13
8.67-9.15	1393	397	3.42±0.10
9.15-9.41	1596	502	3.31±0.09
9.40-9.43	233	70	3.57±0.27
Combined	4052	1141	3.37±0.06

Figure Captions

1. The LENA detector as seen along the beam direction.

2. The acceptance, Q, as a function of center of mass energy.

3. (a)-(c) Visible energy distributions for hadronic events. Three center of mass energy regions are shown. The Monte Carlo results are normalized to the data above the visible energy cuts.
(d)-(f) Charged multiplicity distributions for the same three center of mass regions.
In (a)-(f) τ-pair contributions are included in the Monte Carlo results.

4. The visible energy of Bhabha event tracks. Three energy regions are displayed.

5. Large angle Bhabha angular distributions. The solid curve is the lowest order QED expected distribution.

6. R as a function of center of mass energy. The errors shown are statistical only. The four points labeled ⧗ are from our 1979 data near the $\Upsilon(1S)$.

7. Compilation of results for R in the center of mass region 5.5 to 9.5 GeV. The errors shown are statistical (⊢—●—⊣) and systematic (⊢- -●- -⊣) except for PLUTO (7.7 GeV) and for D-HH-HD-M where the combined errors only are shown.

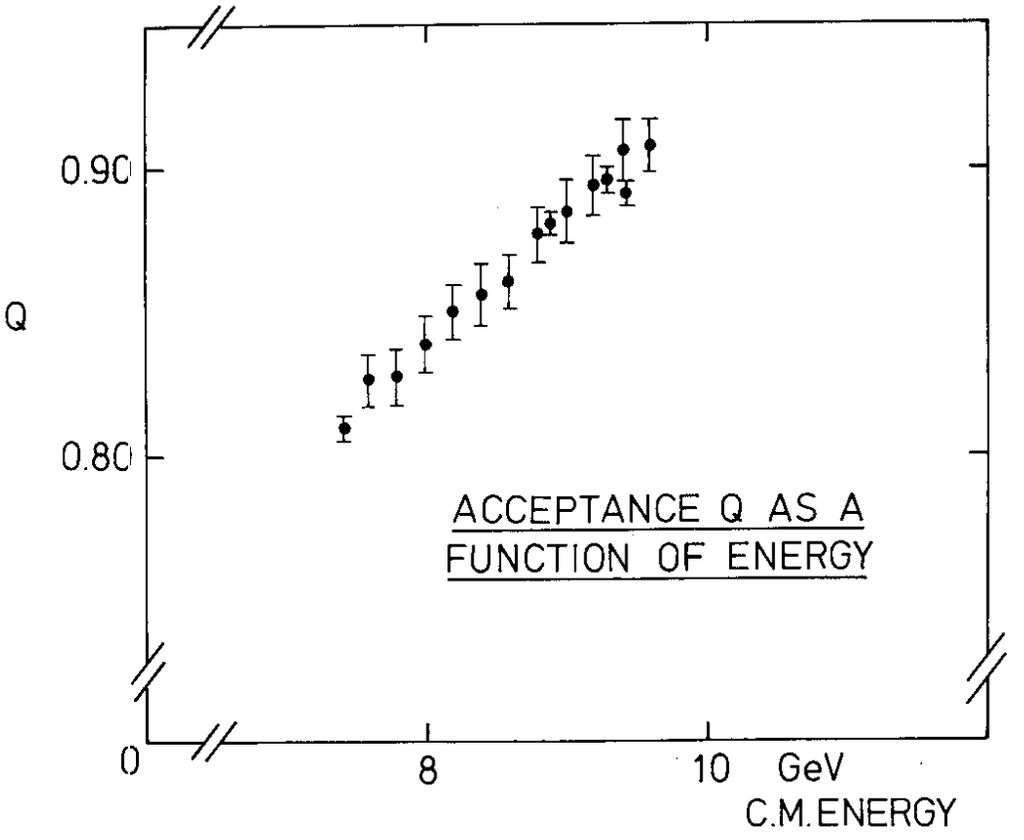

Fig. 2

34241

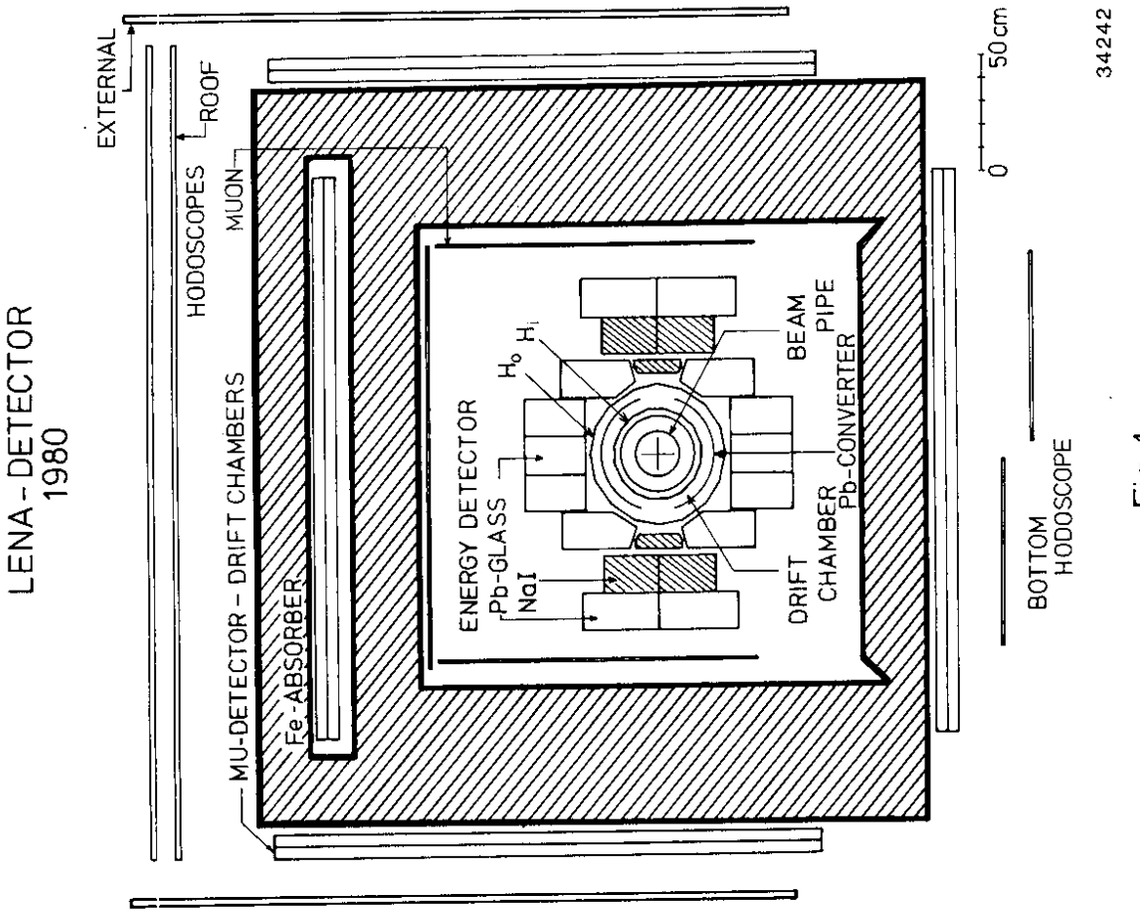

Fig. 1

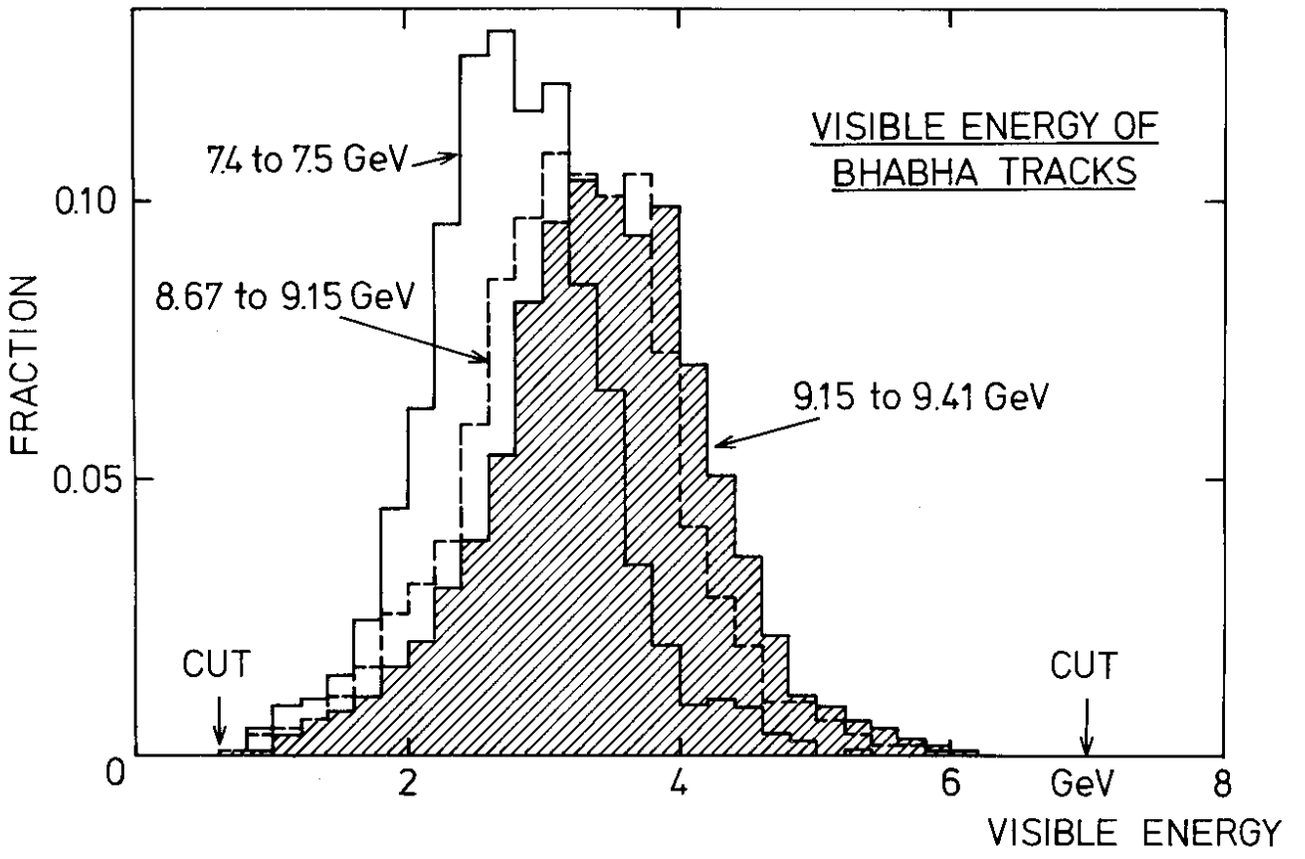

Fig. 4

34240

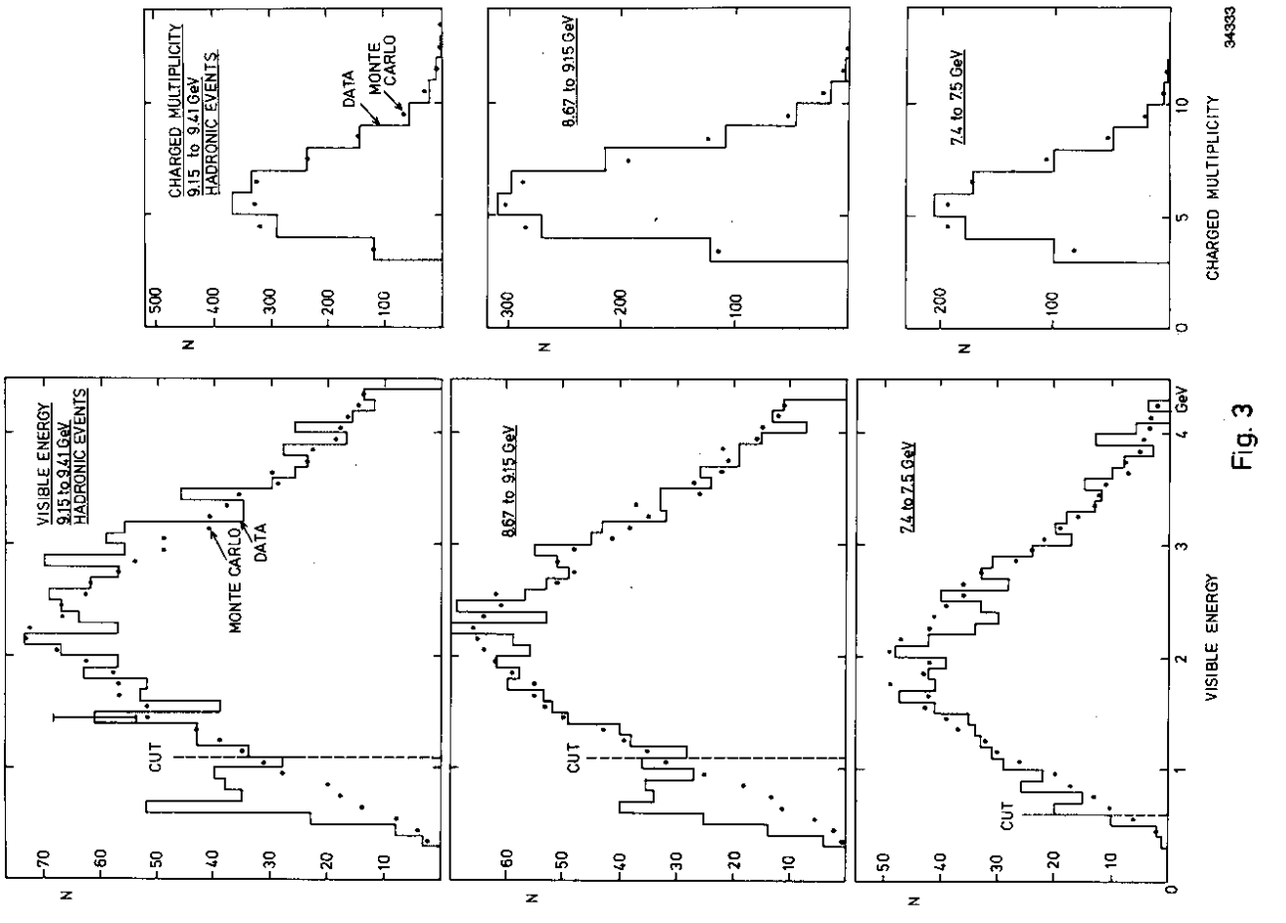

Fig. 3

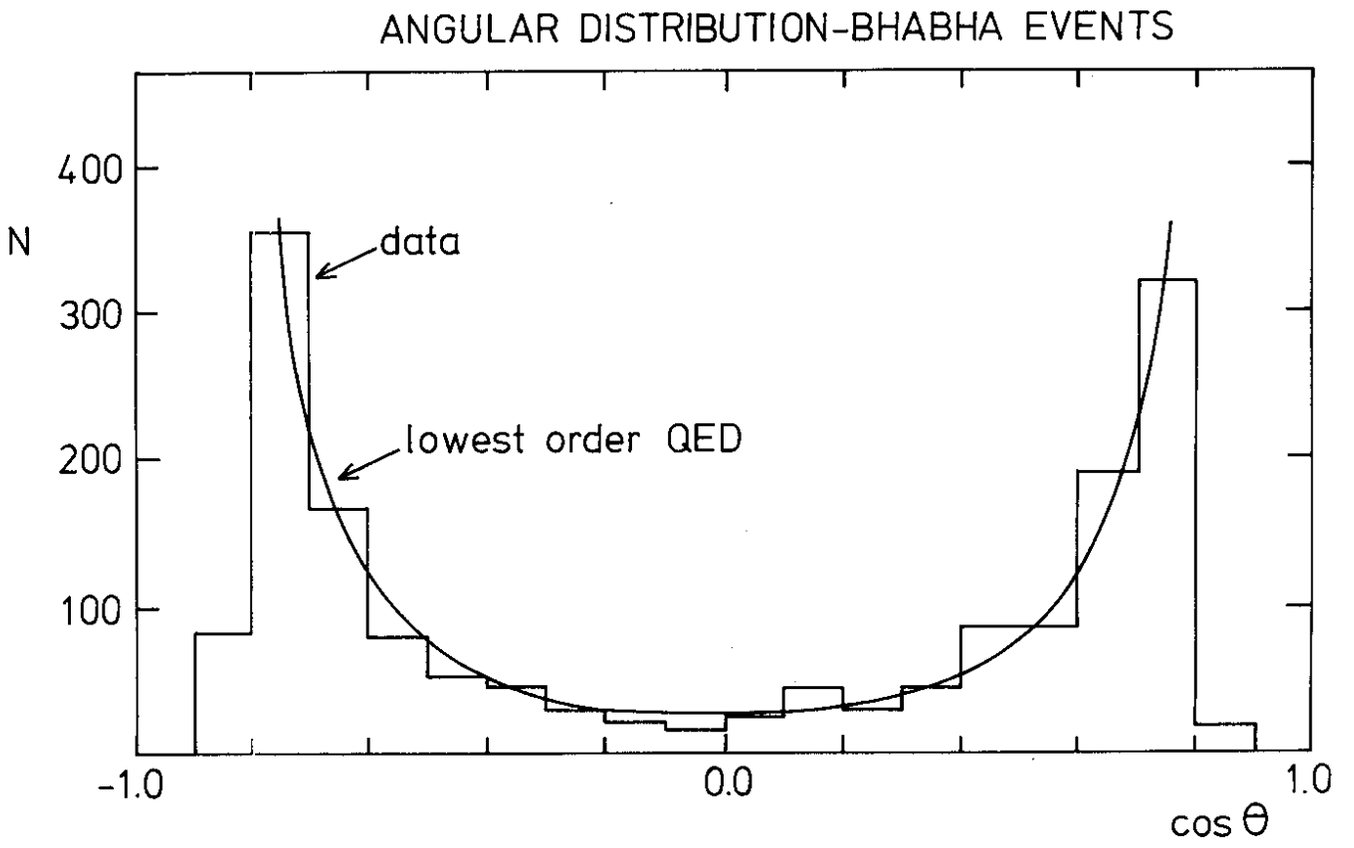
ANGULAR DISTRIBUTION-BHABHA EVENTS
N
400
300
200
100
data
lowest order QED
-1.0
0.0
1.0
cos Θ
34239

Fig. 5

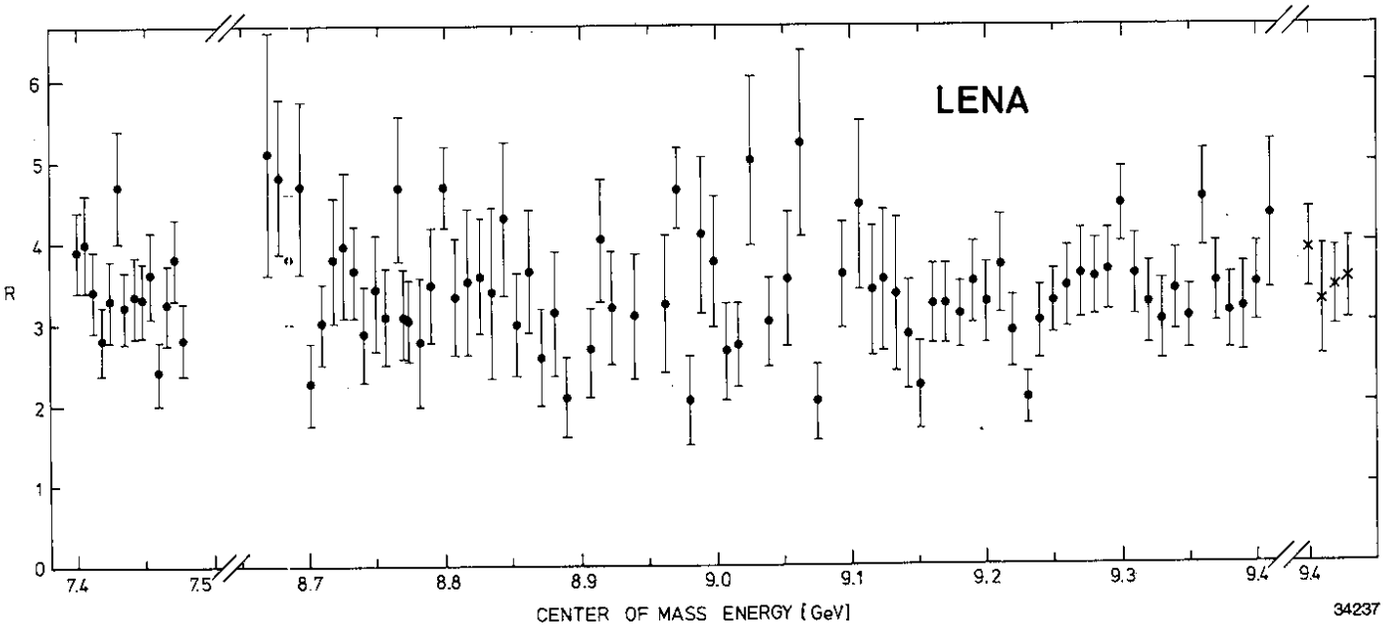
LENA
R
6
5
4
3
2
1
0
7.4
7.5
8.7
8.8
8.9
9.0
9.1
9.2
9.3
9.4
9.4
CENTER OF MASS ENERGY [GeV]
34237

Fig. 6

Appendix.

E_{CM}	N_R	N_B	Q	R	$\Delta R_{stat.}$
7.400	78	246	0.86	3.88	0.50
7.406	58	179	0.86	3.97	0.60
7.412	66	235	0.86	3.39	0.47
7.418	51	218	0.86	2.76	0.43
7.424	56	207	0.86	3.25	0.49
7.430	66	174	0.86	4.72	0.68
7.435	65	242	0.86	3.22	0.45
7.442	54	194	0.86	3.35	0.52
7.448	65	237	0.86	3.30	0.46
7.454	42	142	0.86	3.59	0.63
7.460	49	237	0.86	2.39	0.37
7.466	61	225	0.86	3.26	0.47
7.472	72	238	0.86	3.68	0.49
7.478	47	199	0.86	2.79	0.45
8.670	16	41	0.87	5.09	1.50
8.678	34	92	0.87	4.80	0.96
8.686	30	99	0.87	3.88	0.81
8.694	26	72	0.87	4.68	1.07
8.702	27	146	0.87	2.24	0.47
8.710	46	190	0.87	3.03	0.50
8.718	32	108	0.87	3.78	0.76
8.726	26	84	0.87	3.96	0.89
8.734	38	132	0.87	3.66	0.67
8.742	25	112	0.87	2.76	0.61
8.750	34	124	0.87	3.47	0.67
8.757	34	136	0.87	3.13	0.60
8.766	34	94	0.87	4.67	0.93
8.770	52	211	0.87	3.08	0.48
8.774	43	176	0.87	3.05	0.52
8.782	15	66	0.87	2.81	0.80
8.790	30	108	0.87	3.51	0.72
8.800	31	85	0.87	4.70	0.99
8.808	27	101	0.87	3.36	0.73
8.818	21	75	0.87	3.53	0.87
8.827	33	115	0.88	3.63	0.72
8.838	13	48	0.88	3.40	1.06
8.845	27	80	0.88	4.32	0.96
8.854	27	112	0.88	2.99	0.64
8.863	37	118	0.88	3.99	0.75

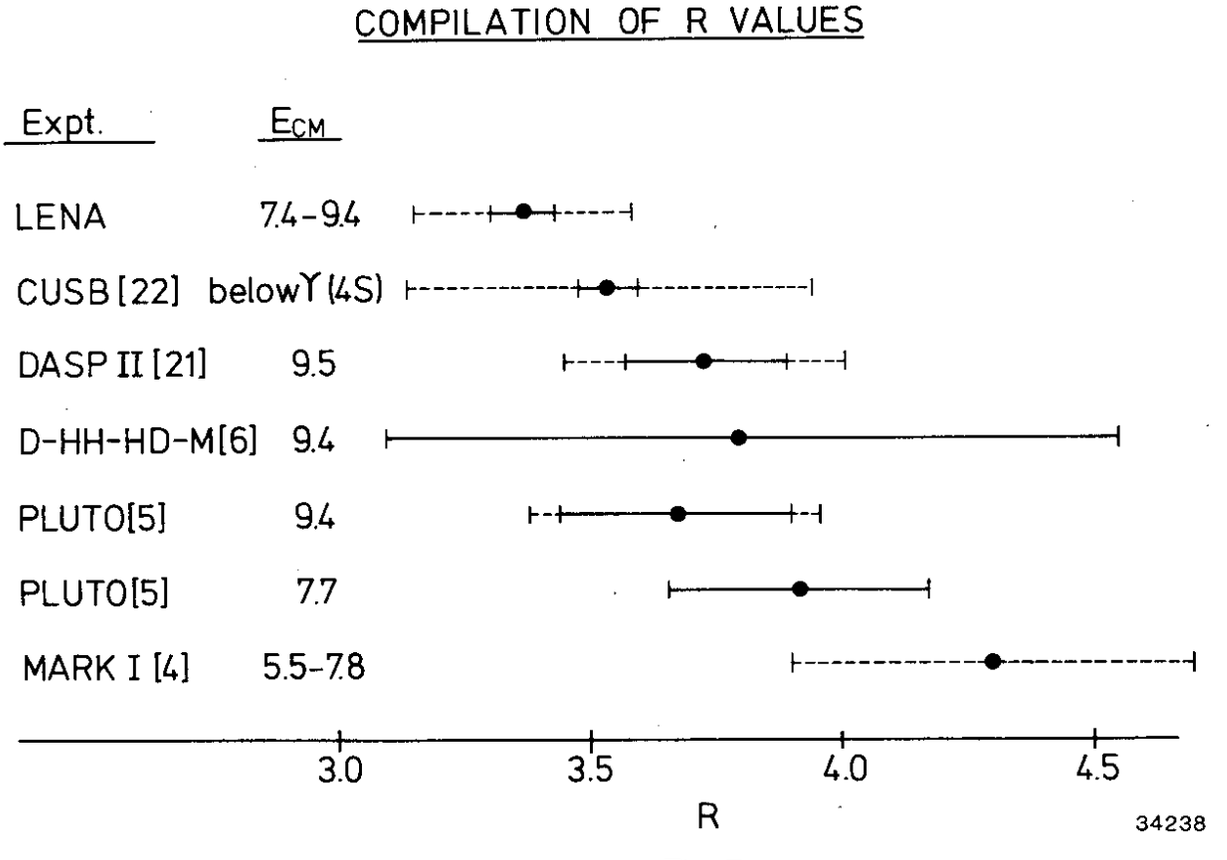

Fig. 7

8.872	23	108	0.88	2.60	0.60
8.881	21	83	0.88	3.15	0.77
8.890	22	124	0.88	2.11	0.49
8.908	25	113	0.88	2.71	0.60
8.916	37	116	0.88	4.05	0.76
8.926	29	109	0.88	3.32	0.69
8.940	20	80	0.88	3.10	0.77
8.962	19	73	0.88	3.24	0.83
8.971	28	77	0.88	4.65	1.03
8.980	16	91	0.88	2.08	0.56
8.989	25	77	0.88	4.11	0.95
8.998	27	90	0.88	3.77	0.83
9.007	24	110	0.88	2.65	0.60
9.016	24	107	0.88	2.74	0.62
9.025	32	82	0.88	5.00	1.04
9.038	41	162	0.88	3.13	0.55
9.052	23	81	0.89	3.54	0.84
9.061	29	71	0.89	5.23	1.15
9.074	22	127	0.89	2.03	0.47
9.093	40	139	0.89	3.59	0.64
9.106	25	71	0.89	4.46	1.04
9.115	24	87	0.89	3.42	0.79
9.124	21	74	0.89	3.53	0.87
9.133	16	59	0.89	3.36	0.95
9.142	22	94	0.89	2.85	0.67
9.150	21	111	0.89	2.24	0.53
9.160	59	223	0.89	3.25	0.48
9.170	57	217	0.89	3.23	0.48
9.180	70	277	0.89	3.10	0.41
9.190	63	226	0.89	3.45	0.49
9.200	55	208	0.89	3.25	0.49
9.210	55	184	0.89	3.71	0.57
9.219	50	211	0.89	2.88	0.45
9.230	49	277	0.89	2.07	0.32
9.240	53	215	0.89	3.00	0.46
9.250	78	295	0.89	3.24	0.41
9.260	60	215	0.90	3.44	0.50
9.270	57	197	0.90	3.57	0.54
9.280	73	254	0.90	3.55	0.47
9.290	68	232	0.90	3.62	0.50
9.300	85	240	0.90	4.44	0.56
9.310	69	239	0.90	3.56	0.49
9.320	54	205	0.90	3.22	0.49
9.330	45	186	0.90	2.93	0.49

9.340	61	222	0.90	3.37	0.49
9.350	76	304	0.90	3.03	0.39
9.360	76	212	0.90	4.48	0.60
9.370	67	237	0.90	3.47	0.48
9.380	54	217	0.90	3.01	0.46
9.390	42	164	0.90	3.11	0.54
9.400	70	248	0.90	3.45	0.47
9.410	29	84	0.90	4.29	0.92
9.400	85	269	0.90	3.91	0.49
9.410	29	109	0.90	3.24	0.68
9.420	57	204	0.90	3.41	0.51
9.430	62	215	0.90	3.53	0.51